

Embedding Samples Dispatching for Recommendation Model Training in Edge Environments

Guopeng Li
USTC
Hefei, China

Hongqiu Ni
USTC
Hefei, China

Yang Xu
USTC
Hefei, China

Haisheng Tan*
USTC
Hefei, China

Zilong Wang
USTC
Hefei, China

Chi Zhang*
Hefei University of Technology
Hefei, China

Xinyue Zhang
USTC
Hefei, China

Han Tian
USTC
Hefei, China

Abstract

Training deep learning recommendation models (DLRMs) on edge workers brings several benefits, particularly in terms of data privacy protection, low latency and personalization. However, due to the huge size of embedding tables, typical DLRM training frameworks adopt one or more parameter servers to maintain global embedding tables, while leveraging the edge workers cache part of them. This incurs significant transmission cost for embedding transmissions between workers and parameter servers, which can dominate the training cycle. In this paper, we investigate how to dispatch input embedding samples to appropriate edge workers to minimize the total embedding transmission cost when facing edge-specific challenges such as heterogeneous networks and limited resources. We develop ESD, a novel mechanism that optimizes the dispatch of input embedding samples to edge workers based on expected embedding transmission cost. We propose HybridDis as the dispatch decision method within ESD, which combines a resource-intensive optimal algorithm and a heuristic algorithm to balance decision quality and resource consumption. We implement a prototype of ESD and compare it with state-of-the-art mechanisms on real-world workloads. Extensive experimental results show that ESD reduces the embedding transmission cost by up to 36.76% and achieves up to 1.74 \times speedup in end-to-end DLRM training.

Keywords

edge computing, embedding cache, recommendation model

1 Introduction

Recommender systems have become essential in daily life, with recommendation models trained on large-scale data to learn user preferences and product characteristics, providing personalized recommendations in e-commerce [22, 57, 64], online entertainment [13, 19, 53], and social media [8, 54, 74] to enhance user experience and drive business growth [10, 67]. In recent years, with the rapid development of mobile and ubiquitous computing, integrating recommender systems into mobile and ubiquitous applications to provide personalized services has become a growing trend, such as energy management recommendations in the Internet of Energy [26, 52],

health advice in health monitoring [50], and destination suggestions in tourism exhibitions [59]. However, conventional recommender systems are typically deployed on cloud servers, which face data privacy concerns and network latency challenges [9, 40, 73, 77]. To deliver recommendation services while ensuring privacy protection and low latency for mobile and ubiquitous applications, training and deploying recommendation models on edge workers is a natural alternative [20, 27, 76].

Deep Learning Recommendation Models (DLRMs), such as WDL [12] and DFM [24], have emerged as highly effective techniques for constructing recommender systems [28]. A typical DLRM follows the *embedding layer* and *multi-layer perceptron (MLP)* paradigm. The embedding layer is practically the embedding tables, transforming the sparse input (e.g., user ID and video ID) into dense vector embeddings [23, 81, 85]. The embedding tables consume a tremendous memory footprint, with each embedding requiring a few KB, and the total memory reaching tens of GBs to TBs. In contrast, the MLP layers, typically ranging from several to hundreds of MBs, are much smaller, and make up the dense model that learns high-order feature interactions and generates the final prediction [83, 87].

When training DLRM on edge workers for mobile and ubiquitous recommendation services, the parameter server (PS) architecture is commonly employed to address the issue of huge embedding tables and the limited memory capacity of edge workers. In the PS architecture, one or more memory-optimized servers (i.e., the parameter servers) maintain the globally embedding tables, while each edge worker caches a portion of embedding tables in its local memory, i.e., *embedding cache*. During DLRM training, workers pull embedding values from the parameter server and push embedding gradients back through the Ethernet, called *embedding transmission*. In production workloads, a single training input sample may involve up to thousands of embeddings [3]. Training DLRM on edge workers suffers from embedding access bottlenecks as each training iteration requires substantial embedding transmission between edge workers and the parameter server [58]. For instance, training WDL [12] with the Criteo Kaggle dataset [1] shows that up to 90% time could be spent on embedding transmission, dominating the training cycle.

In this paper, we aim to reduce the network bandwidth usage, denoted as the *total embedding transmission cost*, in resource-limited

*Corresponding author.

edge environments while simultaneously accelerating DLRM training. Managing the input embedding samples loaded from the data loader for each worker is an effective way to reduce the embedding transmission cost [6, 31, 79]. Specifically, with input samples prefetching in today’s data loaders [43, 49], during the current training iteration, input samples for the next iteration can be proactively dispatched to the appropriate worker to minimize the embedding transmission cost. Intuitively, we may dispatch input samples to the workers that maximize the overall cache hit ratio. However, unlike traditional file caching, embeddings stored on workers during DLRM training are not static, which are continuously updated through synchronization with the parameter server, making the dispatch problem non-trivial. Moreover, the heterogeneous networks and limited resources in edge environments also bring hardness. We summarize the problem challenges as follows.

Cost composition. When training DLRM with the PS architecture, it is crucial that each worker caches the latest versions of embeddings corresponding to the current input samples. If the latest embeddings are not available in the cache, they must be pulled from the parameter server (*miss pull*)¹. For each training iteration, embedding gradients are on-demand synchronized between the workers and the parameter server (*update push*). Additionally, when the embedding cache reaches its capacity, certain embeddings must be evicted to make space for new ones, and their gradients have to be transmitted to the parameter server (*evict push*). Consequently, the embedding transmission cost arises from the *miss pull*, *update push*, and *evict push* operations. Therefore, a mechanism is desired to minimize the total embedding transmission cost rather than merely optimizing the hit ratio.

Heterogeneous networks. When training DLRM in edge environments, there might be significantly lower-bandwidth connections between edge workers and the parameter server compared to the high-bandwidth networks used in cloud data centers (e.g., 100 Gbps Ethernet or InfiniBand). Typically, edge workers connect to the parameter server via heterogeneous networks. For instance, some workers may use 0.5 Gbps connections while others rely on 5 Gbps, leading to varying transmission costs for the embeddings of the same size [36, 48, 62]. Therefore, beyond accounting for the number of miss pull, update push, and evict push operations, it is also necessary to consider the heterogeneous network bandwidths between workers and the parameter server.

Limited resources. In production environments, each iteration typically involves an input batch of thousands of embedding samples, and dispatching these samples to different workers introduces decision-making overhead. In edge environments, where multiple tasks compete for limited resources [29, 38], this overhead must be carefully managed. Furthermore, in the online training scenario considered in this paper, which aims to promptly and accurately capture user interest drift and emerging trends [83, 84], dispatch decisions must be completed within each training iteration to avoid performance degradation. Therefore, when designing the dispatch mechanism, it is crucial to account for both the time and resource consumption of dispatch decision-making in light of the challenges posed by edge environments and online training requirements.

¹This paper employs Bulk Synchronous Parallel (BSP) [18] training for DLRM without sacrificing model accuracy, necessitating the use of the latest embeddings.

Prior works focus on mitigating embedding transmission cost when training DLRM in cloud environments and overlook the consideration for edge-specific challenges [4, 43, 45, 58, 79]. To address the above practical challenges, we propose ESD, a mechanism for dispatching embedding samples to edge workers to reduce the total embedding transmission cost and accelerate DLRM training. ESD assigns an expected transmission cost for training each sample on different edge workers and dispatches samples to appropriate workers to reduce the total embedding transmission cost. To avoid decision time exceeding training time while balancing decision quality and resource consumption, we propose *HybridDis* as the dispatch decision method in ESD, which combines a resource-intensive optimal algorithm with a resource-efficient heuristic algorithm. Our technical contributions are summarized as follows:

- In this paper, we formulate the problem of dispatching embedding samples to minimize the total embedding transmission cost during DLRM training in edge environments, taking into account cost composition, heterogeneous networks and limited resources. To the best of our knowledge, this is the first work specifically focused on minimizing embedding transmission cost in edge environments (Sec. 3).
- We introduce ESD, an embedding sample dispatch mechanism that reduces the total embedding transmission cost by calculating the expected costs for dispatching each embedding sample to different workers. We propose *HybridDis*, a hybrid dispatch decision method within ESD that balances decision quality and resource consumption to address the limited resources challenge (Sec. 4).
- We implement ESD using C++ (including CUDA) and Python to evaluate it through extensive experiments on a testbed with 8 edge workers under real-world workloads. Evaluation results show that compared with LAIA [79], ESD reduces embedding transmissions by up to 36.76% and delivers up to 1.74× performance improvement for end-to-end DLRM training (Sec. 5 and Sec. 6).

2 Background

2.1 Recommender System for Mobile and Ubiquitous Applications in Edge Environments

Recommender systems are now essential in e-commerce, social media, and media applications, offering personalized recommendations that enhance user experience and drive business growth [34, 63]. Traditional recommender systems are cloud-based, where the cloud server trains the model using all user data and pushes recommendation results to users’ devices upon request. Though this paradigm benefits from the infinite computing power, it faces challenges, including high resource consumption [65], dependence on network access for timeliness [39], and user privacy concerns [16, 46, 60, 80], which undermine the sustainability and trustworthiness of cloud-based systems [7]. Furthermore, cloud-based systems often fail to meet the time-sensitive and computational demands of mobile and ubiquitous applications. With the rise of edge computing, there is a trend towards training and deploying recommendation models

in edge environments [20, 27, 76]. This paradigm provides recommendation services while ensuring privacy protection and low latency for mobile and ubiquitous applications such as the Internet of Energy [26, 52, 70], health monitoring [17, 50], and tourism exhibitions [59]. For instance, in the Internet of Energy, recommender systems can suggest energy management solutions and assist in resource allocation. In health monitoring, they provide personalized health advice based on medical history and real-time health information.

For data privacy, this paper achieves privacy by training DLRM on edge workers within a local area network (LAN) isolated from the external internet. This approach keeps private data local, preventing leakage while enabling low-latency recommendation services. Moreover, this paper focuses on online DLRM training. At the system’s initialization stage, the DLRM model is trained on historical data generated by mobile and ubiquitous devices (such as cameras and sensors) on edge workers. To ensure the continuous delivery of high-quality recommendations during the recommendation service, the DLRM model is continuously trained and refined online using streaming data from mobile devices [15, 44, 56, 68, 72, 75]. Overall, this paper focuses on online DLRM training using edge workers and parameter servers connected via a LAN to provide low-latency, privacy-preserving recommendation services for mobile and ubiquitous applications.

2.2 Architecture of Deep Learning Recommendation Model

Deep Learning Recommendation Models, such as WDL [12], DFM [24], DCN [66] and FLEN [11], model the recommendation decision as a problem to predict the probability of a specific event, *e.g.*, the likelihood of a web viewer watching the recommended content (video or music). The general architecture of DLRM mainly consists of an embedding layer, feature interaction layer, and multi-layer perceptron layer (MLP), as shown in Fig. 1. The input of DLRM generally includes both dense and sparse inputs. Dense inputs represent continuous variables, such as age and height, while sparse inputs represent categorical variables, such as user ID and music ID. These are processed by the MLP layer and embedding layer, respectively.

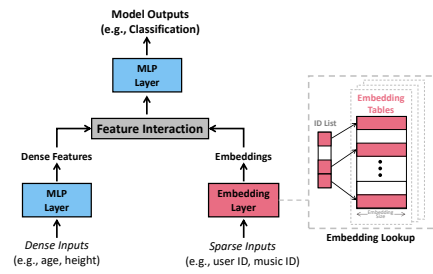


Figure 1: General Architecture of Deep Learning Recommendation Model.

Embedding layer. The embedding layer is practically the embedding tables, where each embedding table represents a categorical feature and each row of this table represents a specific ID (*e.g.*, user

ID or music ID). The embedding table transforms each ID into a fixed size vector with float values that are trainable, *i.e.*, embedding.

MLP layer. The multi-layer perceptron (MLP) layer performs multiple fully connected operations to process dense inputs and handle outputs from the feature interaction layer. It provides a probability of click-through rate (CTR) for a single user-item pair and includes other computation-intensive units, such as batch normalization.

Feature interaction layer. Feature interaction is the process of combining dense and sparse features to capture their complex and nonlinear relationships [83]. The outputs of feature interaction will be processed by the subsequent MLP layer. Operations of feature interaction include averaging, sum, concatenation, *etc.*

2.3 Embedding Transmission Cost in DLRM Training

In DLRM training, different parallelization and communication approaches can be implemented for the embedding and MLP layers. The MLP layers size is small enough to be accommodated by each worker, thus they are replicated across the workers to leverage data parallelism and use AllReduce for communication. On the other hand, embedding layers contribute to $> 99\%$ of the entire model size and can be in the order of several terabytes. Because storing all the embedding tables in a single worker is not feasible, the PS architecture maintains globally shared embeddings in memory-optimized parameter servers, and edge workers cache part of embedding tables in their local memory, *i.e.*, using model parallelism and PS communication [5]. However, this design introduces significant embedding transmission cost when applying bulk synchronous parallel (BSP) training for non-degraded and reproducible model accuracy [51]. BSP training is a parallel computing model that organizes computations into synchronized steps, where each step consists of local computation, communication among workers, and a global synchronization barrier. This ensures all workers stay coordinated and progress together [18]. In each training iteration, workers pull embeddings from the parameter server and push embedding gradients back to the parameter server on demand. In our experiment using the default setting as shown in Sec. 6, the embedding transmission cost dominates the training cycle, which can account for up to 90% of the end-to-end training time. Prior works mitigate embedding transmission cost by reducing the number of embedding transmissions between workers and parameter server [4, 6, 45, 79] or reducing each embedding transmission cost between devices [31, 58, 69, 71]. In this paper, we aim to minimize the total embedding costs during DLRM training in edge environments when facing challenges such as cost composition, heterogeneous networks, and limited resources. This work is similar to the former and orthogonal to the latter.

3 System Model and Problem Formulation

We provide the system model and problem formulation in this section. Commonly used symbols are listed in Table 1.

System. Motivated by training DLRM on multiple edge workers, this work focuses on a system comprising multiple edge GPU workers (workers) and one parameter server (PS). Specifically, the system consists of n workers, $\mathcal{W} = \{w_1, w_2, \dots, w_n\}$. These workers are

connected to the parameter server through Ethernet, typically 5 Gbps or 0.5 Gbps, and are also connected among themselves.

Input Training Samples. In DLRM training, each worker is associated with a data loader, which is a process on the CPU and is responsible for preprocessing the training samples. The data loaders can load training samples from local memory, disk, or network streams. For each training iteration I_t , input generation is usually performed by the data loader, which partitions a batch of inputs into multiple micro-batches for every worker. In this paper, in order to maintain a balanced workload distribution across the workers, we use a fixed m to present the batch size for each worker; thus, for n workers, the total number of input training samples per iteration is $m \times n$. For the $m \times n$ input embedding samples \mathcal{E} , $\forall E_i \in \mathcal{E}$ is an embedding sample, consisting of multiple embedding IDs, $E_i = \{x_1, x_2, x_3, \dots\}$. The ID type feature is the sparse encoding of large-scale categorical information. We use $Emb(x_i)$ to represent the embedding value for x_i .

Embedding Cache. When training DLRM on edge workers, each worker holds a replica of the MLP and uses AllReduce for gradient synchronization during training. The entire embeddings are stored in the global embedding table on the parameter server, while each worker caches a portion of the embedding tables. The workers manage the local cache by transmitting embeddings with the PS to control inconsistencies between the local and global embedding tables. We use r to represent the cache ratio, *i.e.*, the ratio of the number of in-cache embeddings to the total number of embeddings.

Table 1: List of Symbols

Notation	Description
\mathcal{W}	The set of edge servers, $\mathcal{W} = \{w_1, w_2, \dots, w_n\}$
\mathcal{E}_i	The input embedding samples for iteration I_i , $\mathcal{E}_i = \{E_1, E_2, \dots, E_{m \times n}\}$
I_i	The i -th training iteration
m	Batch size for each worker, <i>i.e.</i> , batch size per worker
E_i	An embedding sample, $E_i = \{x_1, x_2, x_3, \dots\}$
x_i	The identifier (ID) for an embedding
$Emb(x_i)$	The embedding vector corresponding to ID x_i
D_{tran}	The data size of an embedding vector
B_w^j	The network bandwidth between worker w_j and the parameter server
T_{tran}^j	The cost for transmitting an embedding between worker w_j and the parameter server, $T_{tran}^j = \frac{D_{tran}}{B_w^j}$

On-demand Synchronization Between Workers and the PS. In BSP training for DLRM, each iteration requires the latest version of embeddings. To maintain consistency, workers transmit embedding

values and gradients with the PS². On-demand synchronization is one method to reduce transmission overhead. Specifically, after iteration I_t , instead of pushing all embedding gradients to the PS, the on-demand push is used in I_{t+1} . For example, if embedding $Emb(x_i)$ is trained on worker w_j during iteration I_t and no other worker ($w' \in \mathcal{W}, w' \neq w_j$) receives samples containing x_i in I_{t+1} , then worker w_j does not need to push the gradient of $Emb(x_i)$ to the PS. Conversely, if other workers require $Emb(x_i)$ in I_{t+1} , worker w_j needs to push $Emb(x_i)$ to the PS, and the other workers pull $Emb(x_i)$ into their caches. Thus, when using on-demand synchronization, the process for each iteration on each worker after receiving training samples from the data loader is as follows: on-demand embedding gradient pushing, pulling latest embeddings not in the local cache, model forward propagation, backward propagation, and dense parameter AllReduce synchronization.

Model Consistency Analysis. In this part, we demonstrate that using on-demand synchronization in BSP does not compromise model accuracy. Accelerating DLRM training under BSP with embedding dispatching can preserve model consistency and thus the exactly same model accuracy. Compared to vanilla distributed training, embedding dispatching introduces two main changes: a specific input embedding samples dispatch mechanism (versus a random dispatch mechanism) and on-demand synchronizations (versus full-set synchronizations). In BSP, on-demand synchronizations ensure that all workers use the latest embedding for the incoming training iteration, which is the same behavior as the vanilla distributed training performs. We prove that the dispatch mechanism under BSP will not affect the training model. Considering a parameter optimizer followed by the SGD algorithm [21], the gradient calculation for model weights y on a given batch of $m \times n$ training samples is expressed as follows:

$$\nabla_y = \frac{1}{m \times n} \sum_{i=1}^{m \times n} \frac{\partial L(\mathcal{E}_i, y)}{\partial y} \quad (1)$$

where \mathcal{E}_i represents the i -th training sample of the batch, and L denotes the loss function. According to Eq. 1, the gradient for the batch is calculated as the sum of the individual gradients for each training sample. Since the individual gradient depends only on input samples and current model weights, which have been synchronized before this iteration begins under BSP, partitioning the batch into n micro-batches does not affect the gradient result:

$$\frac{1}{m \times n} \sum_{i=1}^{m \times n} \frac{\partial L(\mathcal{E}_i, y)}{\partial y} = \frac{1}{m \times n} \sum_{i=1}^n \sum_{j=1}^m \frac{\partial L(E_{ij}, y)}{\partial y} \quad (2)$$

where E_{ij} is the j -th training sample in the i -th micro-batch (for worker w_i). Therefore, any dispatch result generated by any dispatching mechanism preserves the same gradients as in BSP throughout training and converges to the same model.

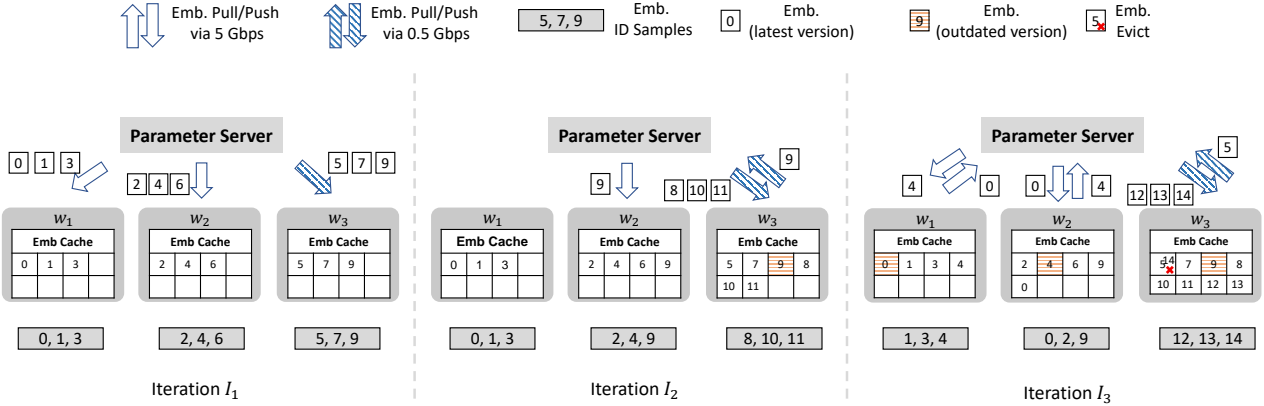


Figure 2: Miss Pull, Update Push, and Evict Push transmission operations in DLRM training.

3.1 System Model

3.2 Problem Formulation

In this work, our goal is to minimize the total embedding transmission cost when training DLRM in edge environments. As shown in Fig. 2, in DLRM training, when using on-demand synchronization, the cost for embedding transmission comes from three embedding transmission operations, *i.e.*, *Miss Pull*, *Update Push*, and *Evict Push*. In Fig. 2, for simplicity, numbers are used to represent embedding IDs and vectors.

- *Miss Pull*: When receiving the training samples from the data loader, the worker should retrieve the necessary embeddings from the local cache or the PS, a process known as embedding lookup. If the required embedding is available with the latest version, there is no need to pull the embedding from the PS. In the context of cache, this is a cache hit. Conversely, if the required embedding is absent or outdated, it must be pulled from the PS, resulting in a cache miss and incurring additional transmission cost (*Miss Pull*), as shown for embeddings $Emb(x_8)$, $Emb(x_9)$, $Emb(x_{10})$, and $Emb(x_{11})$ in iteration I_2 in Fig. 2.
- *Update Push*: When using on-demand synchronization, the gradient push occurs at the start of each iteration rather than at its end. Upon receiving the training samples, if some embeddings were trained on other workers in the previous iteration, the other worker should *Update Push* the embedding gradient to the parameter server. For example, in iteration I_2 in Fig. 2, worker w_3 should push the embedding gradient of x_9 to the PS for training on worker w_2 .
- *Evict Push*: In addition to the *Miss Pull* caused by cache misses and the *Update Push* introduced by on-demand synchronization, if the worker's cache is full, it needs to evict embeddings to make room for the current training iteration. During eviction, if unsynchronized embeddings are evicted, their gradients must be updated to the parameter server. This process is referred to as *Evict Push* (*e.g.*, the eviction of $Emb(x_5)$ in iteration I_3 in Fig. 2).

The goal of this paper is to minimize the total embedding transmission cost across all iterations. We assume that the data size for each embedding pull and push is the same, denoted as D_{tran} . For iteration I_t , the number of embedding transmissions is T_{num}^t . Given a network bandwidth of B_w , the cost for each transmission operation is $T_{tran} = \frac{D_{tran}}{B_w}$.

Problem P:

$$\text{minimize} \quad \sum_{\text{for all iterations}} T_{num}^t \times T_{tran} \quad (3)$$

4 Mechanism Design

In this section, we first demonstrate the process of input embedding samples dispatching in ESD. Second, we introduce how to calculate the expected transmission cost in Sec. 4.2. Then, given the limited resources in edge environments, we propose HybridDis, a hybrid dispatch decision method that balances solution quality and resource consumption in Sec. 4.3.

4.1 Process of embedding samples dispatching in ESD

Fig. 3 presents an overview of the embedding samples dispatching process in ESD. Specifically, at the start of training iteration I_t , ESD makes dispatch decisions for iteration I_{t+1} based on the input embedding samples for iteration I_{t+1} and the current states (cached or not, the latest version or not) of the cached embeddings on each worker. Additionally, based on the dispatch decision and the current states of the cached embeddings on each worker, ESD can generate the update pushing plan for each worker for iteration I_{t+1} , which is omitted in Fig. 3. Due to this paper focusing on online DLRM training, the dispatch decision time for iteration I_{t+1} should be hidden within the training time of I_t to ensure that embedding sample dispatching can reduce the training time. The above dispatch process is executed locally on each worker, rather than by a centralized orchestrator, to avoid the overhead of distributing dispatching decisions.

To reduce the embedding transmission cost, for input embedding samples \mathcal{E}_i , we assign an expected transmission cost c_i^j for each embedding sample E_i ($E_i \in \mathcal{E}_i$) training on worker w_j , and

²In this paper, we refer to both embedding value and gradient transmission as embedding transmission, which includes embedding value pull and embedding gradient push.

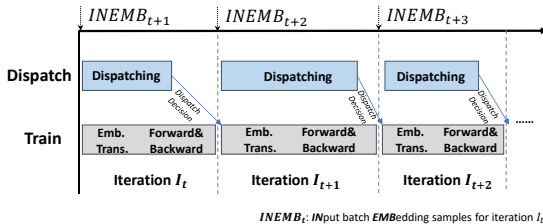


Figure 3: Overview of embedding samples dispatching process in ESD.

dispatch embedding samples to the workers to minimize the total embedding transmission cost. When dispatching input embedding samples based on the expected transmission cost, decision-making consumes the resources of edge workers, which are limited and subject to competition from multiple tasks. ESD incorporates a hybrid dispatch decision method *HybridDis*, which combines a resource-intensive optimal algorithm (Opt) and a heuristic algorithm (Heu) to balance solution quality (*i.e.*, the total embedding transmission cost) and resource consumption. For example, $ESD(\alpha = 0.25)$ indicates that 25% of the input embedding samples use Opt for dispatch decisions, while the remaining 75% use Heu. We analyze the dispatch error when using Heu, and partition input embedding samples to different dispatch decision methods by $\min_2 - \min$, where \min_2 and \min represent the second minimum and minimum costs, respectively, for training embedding sample E_i on different workers.

4.2 Expected Transmission Cost

This subsection demonstrates the method to calculate the expected transmission cost.

Since the embedding states of the embedding cache on each worker are visible, and today's data loaders can prefetch embedding samples for the next iteration, as shown from Line 3 to Line 9 in Alg. 1, we calculate the expected transmission cost of dispatching each embedding sample to each worker. We introduce the calculation method through an example. Considering the start of iteration I_t , we begin calculating the expected transmission costs for embedding samples for the next iteration, *i.e.*, I_{t+1} . If the input embedding sample $E_i = \{x_1, x_2, x_3, \dots\}$ is dispatched to worker w_j for training, for embedding value $Emb(x_i)$ of x_i , if the latest version of $Emb(x_i)$ is not in w_j 's cache, a Miss Pull transmission operation is required, with a cost of T_{tran}^j (Line 7). Additionally, if the latest version of embedding $Emb(x_i)$ exists on other workers during the current iteration I_t , under on-demand synchronization, the other worker ($w_{j'}$) needs to push $Emb(x_i)$ to the parameter server, thus $c_i^j + = T_{tran}^{j'}$, *i.e.*, the cost of worker $w_{j'}$ pushing the embedding to the parameter server is added (Line 9). This way, for iteration I_{t+1} , we obtain the expected transmission cost of dispatching each embedding sample to different workers and store the expected transmission cost in the cost matrix C . For Line 6 and Line 8 in Alg. 1, *in* indicates that the latest version of $Emb(x_i)$ is available in the embedding cache of the edge worker, while *not in* means it is not.

Moreover, training DLRM in edge environments faces heterogeneous network bandwidth between edge workers and the PS, *i.e.*, different workers have varying network bandwidths (B_w^j), leading to different T_{tran}^j . For instance, for iteration I_2 in Fig. 2, the bandwidth between w_2 and the PS is 5 Gbps, whereas between w_3 and

the PS, it is only 0.5 Gbps. As a result, the cost to pull $Emb(x_8)$ from the PS to w_3 is ten times the cost to pull $Emb(x_9)$ to w_2 , *i.e.*, $T_{tran}^3 = 10 \times T_{tran}^2$.

Algorithm 1: ESD

Input: Input embedding samples \mathcal{E} for one iteration, $|\mathcal{E}| = m \times n$, workers \mathcal{W} , cost matrix C .

Output: Dispatch decision (*Decision*).

```

1 Initialize Decision;
2 Initialize all elements in  $C$  with 0;
3 for  $E_i$  in  $\mathcal{E}$  do
4   for  $w_j$  in  $\mathcal{W}$  do
5     for  $x_i$  in  $E_i$  do
6       if  $Emb(x_i)$  for  $x_i$  not in  $w_j$  then
7          $c_i^j + = T_{tran}^j$ ;
8       if  $Emb(x_i)$  for  $x_i$  in  $w_{j'}$  then
9          $c_i^j + = T_{tran}^{j'}$ ;
10 Decision = HybridDis ( $C$ );
11 return Decision.

```

4.3 HybridDis

After calculating the expected transmission cost for training each embedding sample on each worker and obtaining the cost matrix C , this section focuses on designing a decision method to determine the dispatch decision that minimizes the total embedding transmission cost.

In resource-limited edge environments, ensuring the time required to derive a dispatch decision remains shorter than the training time per iteration poses a challenge. We first identify the limitation of sequentially executing the Hungarian algorithm on CPU, which results in excessive solution time. We then briefly analyze the feasibility of parallelizing the Hungarian algorithm using CUDA programming (Opt). To balance solution quality (*i.e.*, the total embedding transmission cost) and resource consumption, we introduce a resource-efficient heuristic method Heu. While Opt delivers optimal dispatch decisions with high resource consumption, we propose a hybrid dispatch method *HybridDis* that combines Opt and Heu. In *HybridDis*, the dispatch error of Heu is a partitioning criterion for assigning portions of the cost matrix to Opt and Heu.

The problem of finding the optimal dispatch decision of cost matrix C that minimizes the total embedding transmission cost can be solved as an assignment problem using the Hungarian algorithm [30]. When the batch size per worker is m , and the number of workers is n , the cost matrix C has dimensions of $(m \times n) \times n$. To accommodate the constraint of m batches per worker, we expand each column of C to m columns, resulting in a square matrix C' with order k ($k = m \times n$), which serves as input to the Hungarian algorithm. The Hungarian algorithm has a time complexity of $O(k^3)$ [33]. As demonstrated in Table 2, sequential execution on CPU shows that when the batch size per worker increases from 32 to 1024, the execution time escalates from 9 milliseconds to 134.986 seconds. This significant latency exceeds the training time per iteration, violating our requirement that the dispatch decision for iteration I_{t+1}

should be computed within the training time of iteration I_t to avoid increasing the end-to-end training time. Our analysis reveals that the Hungarian algorithm contains several inherently parallel components, including subtracting minimum values from each row or column in initial reduction, zero-element covering in initial matching, and matrix updates during matrix adjustment [41]. Therefore, we implement a CUDA-based parallel version of the Hungarian algorithm to ensure the dispatch decision latency remains within the training time constraints. The effectiveness of this parallelization is evidenced by the execution times shown in Table 2. For a comprehensive description of the Hungarian algorithm, please refer to [33, 47].

Table 2: Execution time (millisecond) comparison between serial and parallel implementations of Hungarian algorithm for different batch size per worker (BPW) when using 8 workers.

Batch Size Per Worker	32	64	128	256	512	1024
Serial	9	62	528	3360	50976	134986
Parallel	21	28	82	186	811	1385

Algorithm 2: HybridDis

Input: Input embedding samples \mathcal{E} , $|\mathcal{E}| = m \times n$, workers \mathcal{W} , $\text{maxworkload} = m$, cost matrix C , α , workload list $\text{workload}[1 \dots n]$.

Output: \mathcal{D} . // Dispatch Decision

- 1 Initialize $\text{workload}[1 \dots n]$ with zeros;
- 2 Calculate $\min_2 - \min$ of each row in C ;
- 3 Sort rows in C by $\min_2 - \min$ in descending order;
- 4 $C_{\text{heu}} \leftarrow$ rows of C from $\lceil |\mathcal{E}| \times \alpha \rceil$ to $|\mathcal{E}|$;
- // Preserve initial row numbering
- 5 $C_{\text{opt}} \leftarrow$ rows of C from 0 to $\lfloor |\mathcal{E}| \times \alpha \rfloor$;
- 6 Expand each column to $\lfloor \text{maxworkload} \times \alpha \rfloor$ columns of C_{opt} ;
- 7 $\mathcal{D} = \text{Opt}(C_{\text{opt}})$;
- 8 $\text{maxworkload} = \text{maxworkload} - \lfloor \text{maxworkload} \times \alpha \rfloor$;
- 9 **for** row_i in C_{heu} **do**
- 10 **while** True **do**
- 11 Select the minimum value c_i^j in row_i ;
- 12 **if** $\text{workload}[j] < \text{maxworkload}$ **then**
- 13 Dispatch E_i to worker w_j ;
- 14 Add dispatch decision E_i to w_j into \mathcal{D} ;
- 15 $\text{workload}[j] += 1$;
- 16 **break**;
- 17 **else**
- 18 Exclude c_i^j from the selection in row_i ;
- 19 **return** \mathcal{D} .

In edge environments, although the Hungarian algorithm can provide the optimal dispatch decision to minimize the total embedding transmission cost for each iteration, implementing the

Hungarian algorithm using CUDA consumes inherently limited and competing GPU resources. To balance the dispatch decision quality and the resource consumption, as shown in Alg. 2, we propose HybridDis, a hybrid method to dispatch the input embedding samples to edge workers, which combines the Hungarian algorithm (Opt) and the heuristic algorithm (Heu) to make dispatch decision.

Line 9 to Line 18 in Alg. 2 show the heuristic method Heu. For dispatching input embedding samples to workers, since we have the cost matrix C , where row_i represents n expected embedding cost for dispatching E_i to n workers, Heu greedily dispatches E_i to the worker with the lowest expected cost unless the worker reaches its maximum workload. For example, if c_i^j is the minimum value in row_i of C , then E_i is dispatched to w_j . In this paper, for each iteration, to avoid imbalance among different workers, each worker processes m embedding samples, i.e., m is the maxworkload of each worker. While this approach is not optimal, according to Theorem 1, the worst-case dispatch error is $\min_{\lfloor i/m \rfloor + 1} - \min$ for row_i , $\min_{\lfloor i/m \rfloor + 1}$ and \min represent the $\lfloor i/m \rfloor + 1$ -th minimum and the minimum values in row_i , respectively.

To balance decision quality and computational efficiency, HybridDis employs the $\min_2 - \min$ metric as the partitioning criterion for each row. Specifically, we assign a fraction α ($0 \leq \alpha \leq 1$) of rows with the highest $\min_2 - \min$ values to Opt, while the remaining rows are processed by Heu (Line 2 to Line 5). This ensures that embedding samples with larger potential dispatch errors are handled by the optimal solver. It is worth noting that the partitioning criterion is flexible and can be adapted based on specific requirements. Alternative metrics such as $\min_3 - \min$, $\min_3 - \min_2$, or row-wise averages can be employed, depending on the data distribution patterns observed in practical DLRM training scenarios.

Theorem 1. *When using Heu, for row_i , the worst-case dispatch error is $\min_{\lfloor i/m \rfloor + 1} - \min$. $\min_{\lfloor i/m \rfloor + 1}$ and \min represent the $\lfloor i/m \rfloor + 1$ -th minimum and the minimum values in row_i , respectively.*

PROOF. For the cost matrix C , with $m \times n$ rows and n columns, each column can be dispatched up to m times. For row_i ($0 \leq i \leq m-1$), the worst-case error is 0, as no column will reach maxworkload . For row_i ($m \leq i \leq 2m-1$), the worst-case scenario is that all row_i ($0 \leq i \leq m-1$) are dispatched to the same worker w_{u^1} , and in row_i ($m \leq i \leq 2m-1$), the minimum values are all $c_i^{u^1}$. Since the column representing worker w_{u^1} has already reached maxworkload , for row_i ($m \leq i \leq 2m-1$), we can only choose \min_2 . For row_i ($2m \leq i \leq 3m-1$), similarly, if all row_i ($0 \leq i \leq m-1$) are dispatched to the same worker w_{u^1} and all row_i ($m \leq i \leq 2m-1$) are dispatched to the same worker w_{u^2} , for row_i ($2m \leq i \leq 3m-1$), their minimum values and \min_2 are both located in $c_i^{u^1}$ or $c_i^{u^2}$. But since w_{u^1} and w_{u^2} have both reached maxworkload , row_i ($2m \leq i \leq 3m-1$) can only choose \min_3 . By this logic, for row_i (i.e., embedding sample E_i), the worst-case dispatch error is $\min_{\lfloor i/m \rfloor + 1} - \min$. $\min_{\lfloor i/m \rfloor + 1}$ and \min represent the $\lfloor i/m \rfloor + 1$ -th minimum and the minimum values (costs) in row_i , respectively. \square

5 Implementation

We implement a prototype of ESD on top of HET [45] with C++ and Python. Besides the design described in Sec. 4, ESD maintains cache

snapshots of all workers to provide information on embedding locations. These cache snapshots are used to calculate expected transmission cost, and updated at the end of the dispatch based on the dispatch result. We replace the data loader implementation in HET, the data loader in ESD returns embedding samples and on-demand synchronized embedding indexes as sparse inputs. To support input prefetching without interfering with the training process, ESD is launched by dedicated threads, and the dispatching decisions of ESD are transmitted to the data loader via shared memory. Additionally, we use CUDA to parallelize the initial reduction, initial matching, and matrix adjustment steps of the Hungarian algorithm.

6 Evaluation

We evaluate the performance of ESD using typical workloads as listed in Table 3. Compared with LAIA, the state-of-the-art mechanism that reduces the training time by reducing the number of embedding transmissions, ESD achieves up to a $1.74\times$ speedup and reduces embedding transmission cost by up to 36.76%. Through sensitivity analysis on the batch size per worker, cache ratio, and embedding size, ESD consistently outperforms baselines. All experiments are conducted five times, and the average results are reported.

6.1 Evaluation Settings

Testbed. Both workers and PS are equipped with a 28-core Intel Xeon Gold 6330 CPU at 2.0 GHz and 64 GB (500 GB in PS) of RAM. Each worker is equipped with a Nvidia 4090 GPU. These workers and the PS are connected via 5 or 0.5 Gbps Ethernet. All machines run Ubuntu 18.04, Python 3.8, CUDA 11.3, cuDNN 8.2.0, NCCL 2.8, and OpenMPI 4.0.3.

Unless mentioned otherwise, our experimental setup consists of 8 edge workers and 1 PS. Four workers are connected to the PS via 5 Gbps Ethernet, and the other four via 0.5 Gbps Ethernet. The batch size per worker is 128 and the embedding size is 512. Each worker contains an embedding cache that can house 8% of the PS-side embedding tables by default.

Baselines. We compare ESD with the following mechanisms.

- **HET** [45]: HET is a mechanism that enables embedding caching under the PS architecture by tracking embedding versions to tolerate bounded staleness. When retrieving an embedding, the local version is compared with the PS version, and if the difference exceeds a threshold, the embedding is pulled from the PS. This same method applies to gradient synchronization.
- **FAE** [4]: FAE is designed with static caching. Cached embeddings are profiled and fixed offline before training. All workers in FAE cache the same embeddings, and they synchronize all cached embeddings using AllReduce.
- **LAIA** [79]: LAIA is designed for scheduling embeddings among multiple cloud workers. LAIA calculates a score to quantify the relevance between every input sample and worker and allocates each input to the worker with the highest score.

HET and FAE reduce the embedding transmissions by compromising model accuracy and are orthogonal to ESD, and we adopt

BSP training in HET and FAE. In this section, ESD is used to represent the mechanism regardless of the value of α . ESD($\alpha = 1$), ESD($\alpha = 0.5$), ESD($\alpha = 0.25$), ESD($\alpha = 0.125$), and ESD($\alpha = 0$) represent the mechanisms with different α .

Workloads. We use three real-world models with representative datasets for end-to-end experiments, as listed in Table 3. We exclude the first 10 iterations for warm-up and report the performance for the subsequent iterations. We do not include training accuracy results because ESD can preserve a consistent model accuracy, as analyzed in Sec. 3.1.

Table 3: Workloads for evaluation.

Workload	Model	Dataset
S1	WDL [12]	Criteo Kaggle [1]
S2	DFM [24]	Avazu [2]
S3	DCN [66]	Criteo Sponsored Search [61]

Metrics. The metrics used to evaluate the performance of the mechanisms are Iterations per Second (ItpS), and the total embedding transmission Cost (Cost). To facilitate comparisons, the ItpS of LAIA is used as the reference for describing, with the performance improvements of other mechanisms expressed as a ratio to this reference.

$$\text{Speedup of A} = \frac{\text{ItpS(A)}}{\text{ItpS(LAIA)}}.$$

LAIA is also used as a reference for embedding transmission cost reduction.

$$\text{Cost Reduction of A} = \frac{\text{Cost(LAIA)} - \text{Cost(A)}}{\text{Cost(LAIA)}}.$$

6.2 Overall Performance

We first evaluate the overall performance of speedup and transmission cost reduction of ESD($\alpha = 1$), ESD($\alpha = 0.5$) and ESD($\alpha = 0$) and compare it with baselines under the default setting. Fig. 4a shows the training speedup of ESD ESD($\alpha = 1$), ESD($\alpha = 0.5$) and ESD($\alpha = 0$) over baselines across different workloads. We observe that ESD can achieve $1.03\times$ to $1.74\times$ speedup compared to LAIA (used as the reference and not shown in Fig. 4). Specifically, we find that as α decreases, the speedup also decreases. This is reasonable because a larger α means more embedding samples are handled by Opt, resulting in lower embedding transmission cost per iteration. As shown in Fig. 4b, ESD($\alpha = 1$) reduces transmission cost by up to 36.76% compared to LAIA, while ESD($\alpha = 0.5$) and ESD($\alpha = 0$) achieve 10.81% and 7.03% reductions, respectively. Our experimental results indicate that FAE and HET consistently underperform compared to LAIA. Therefore, to focus on the improvements of ESD over LAIA, we omitted the results of FAE and HET in subsequent experimental analyses.

6.3 Hit Ratio and Ingredient of Transmission Operations

To explore the reasons that affect the performance of these mechanisms, we show the hit ratio and the ingredient of embedding transmission operations in Fig. 5.

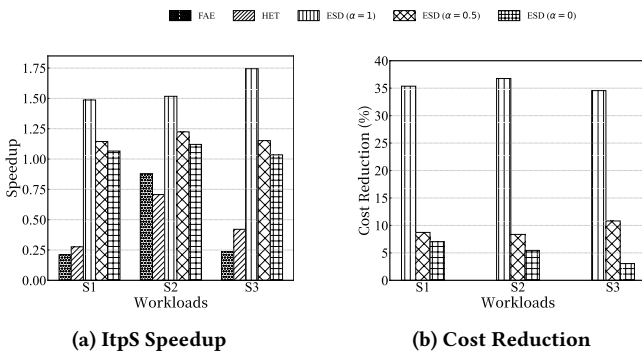


Figure 4: Overall performance.

When we assume x_i exists in the input embedding samples for worker w_j , if the latest version of $Emb(x_i)$ is already cached in w_j 's embedding cache, it is considered a *hit*. The hit ratio is defined as the fraction of embedding lookups that hit the cache relative to the total number of lookups. We present the hit ratio for LAIA, ESD($\alpha = 1$), ESD($\alpha = 0.5$), and ESD($\alpha = 0$) in Fig. 5a. Compared to LAIA, ESD does not achieve a higher hit ratio. However, as shown in Fig. 4, ESD reduces the cost and accelerates end-to-end training compared to LAIA. This is expected, as discussed in Sec. 1, since embedding transmission cost arises not only from embedding misses but also from update push and evict push operations. Therefore, a higher hit ratio does not necessarily lead to reduced embedding transmission.

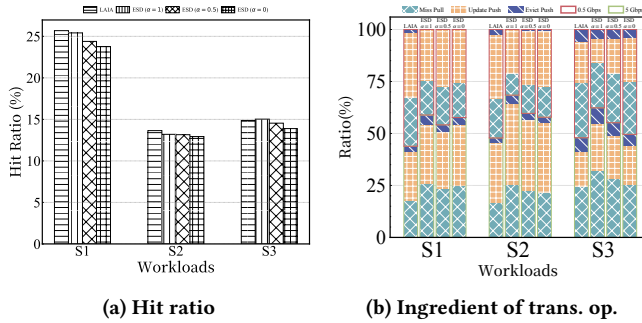


Figure 5: Hit ratio and Ingredient of transmission operations.

Fig. 5b illustrates the ingredient of embedding transmission operations for different mechanisms, *i.e.*, the proportions of miss pull, update push, and evict push operations in the total transmission operations. In each bar chart, the bottom three sections represent the results for 5 Gbps workers, while the upper sections correspond to 0.5 Gbps workers³. As Fig. 5b shows, compared to LAIA, ESD increases the proportion of operations on 5 Gbps workers across all three workloads, whereas in LAIA, the proportion of operations on 5 Gbps workers is smaller than that on 0.5 Gbps workers. This demonstrates that ESD effectively considers the heterogeneous networks. Fig. 5b also shows that miss pull and update push account for over 90% of embedding transmission operations, while evict push contributes less than 10%.

³For simplicity, “5 Gbps worker(s)” refers to workers connected to the parameter server via 5 Gbps Ethernet, and “0.5 Gbps worker(s)” similarly refers to workers connected via 0.5 Gbps Ethernet.

6.4 Cost Reduction and GPU Resource Consumption

Due to limited resources on edge workers, this paper proposes HybridDis, a hybrid method to make the input embedding samples dispatch decision, with α representing the proportion dispatch using Opt. As shown in Fig. 6, when α is 1, 0.5, 0.25, 0.125, and 0, with batch sizes per worker of 128 and 256, we demonstrate the cost reduction and the GPU resource consumption (represented by GPU Utilization). For ESD($\alpha = 0$), the GPU utilization is 0. When the batch size per worker is 128, as shown in Fig. 6a, under different workloads, a larger α results in greater cost reduction and higher GPU utilization. On S1, ESD($\alpha = 1$) achieves the maximum cost reduction, and the GPU utilization is 74.89%. When the batch size per worker is 256, as shown in Fig. 6b, ESD can reduce the embedding transmission cost by up to 40.84%. For ESD($\alpha = 0.5$), when the batch size per worker is 128, GPU utilization ranges from 17.59% to 19.72% across three workloads, while for a batch size of 256, GPU utilization ranges from 50% to 59%. Overall, a larger α results in greater cost reduction and higher GPU utilization. The setting of α depends on the limited GPU resources and the competition among multiple tasks on edge workers. However, even with $\alpha = 0$, ESD can still reduce the transmission cost relative to LAIA.

It is important to note that accurately measuring GPU resource consumption is a challenging issue in computer systems [14, 55]. In Fig. 6, this paper uses the command nvttop to obtain the GPU utilization, which only provides a coarse-grained measure of GPU utilization. Moreover, GPU utilization of ESD in Fig. 6 is measured by executing ESD independently on the GPU rather than during the training process. In fact, when training on workload S3 with batch size per worker is 128, the GPU utilization observed via nvttop is approximately 55% when ESD($\alpha = 1$) is executed concurrently during training, whereas the GPU utilization when running ESD($\alpha = 1$) alone, as shown in Figure 7(a), is approximately 58%. Overall, the GPU utilization shown in Fig. 6 is intended to illustrate that as α decreases, the GPU resources used are reduced. However, the displayed values do not represent the actual GPU resource consumption; that is, ESD($\alpha = 1$) does not actually consume up to 70% of GPU resources as Fig. 6 shows.

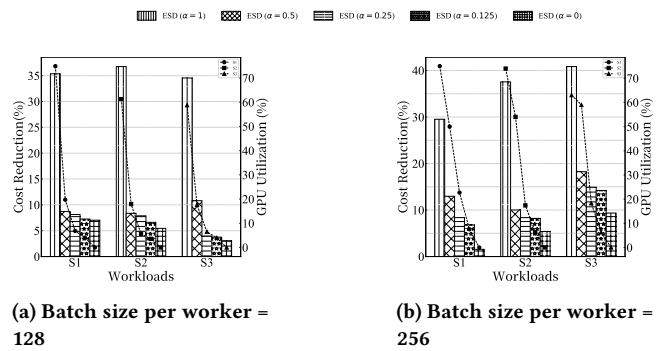


Figure 6: Cost reduction and GPU utilization.

6.5 Sensitivity Analysis

Next, we explore the performance of ESD when the batch size per worker, cache ratio, and embedding size change. Additionally, we assess the performance of ESD with four workers and homogeneous networks (same bandwidth) between workers and the parameter server. When one setting changes, other settings remain at their default setting, in this part, we mainly focus on workload S2.

Batch Size Per Worker.

As Fig. 7 shows, to investigate the impact of batch size per worker, we vary it from 64 to 512 and present the speedup and the cost reduction. When the batch size per worker increases from 64 to 256, the speedup trends for ESD($\alpha = 1$), ESD($\alpha = 0.5$), and ESD($\alpha = 0.25$) are increasing, reaching up to $1.54\times$. However, when the batch size per worker increases from 256 to 512, the speedup for ESD($\alpha = 1$), ESD($\alpha = 0.5$), and ESD($\alpha = 0.25$) does not surpass that at 256 (although it remains above 1). This is because increasing the batch size per worker increases the decision-making time for ESD($\alpha = 1$) and ESD($\alpha = 0.5$), and the solution quality of ESD($\alpha = 0$) decreases with the larger batch size per worker. Thus, the speedup for all three mechanisms declines. For the cost reduction of each mechanism, as the batch size per worker increases, the general trends of cost reduction and speedup are similar. When the batch size per worker increases from 256 to 512, although ESD($\alpha = 1$) achieves greater cost reduction, the increased decision-making time reduces the speedup from 1.54 to 1.23 .

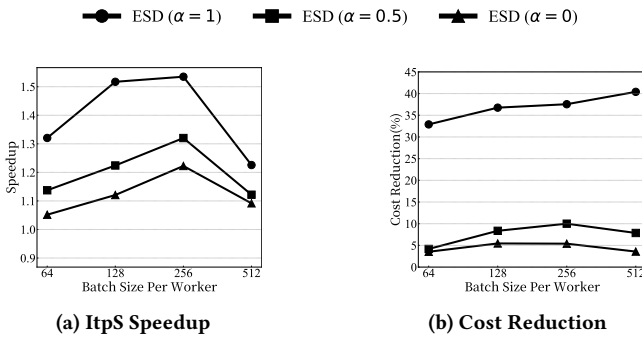


Figure 7: Impact of batch size per worker.

Cache Ratio. We show the result of the impact of cache ratio in Fig. 8. The cache ratio, *i.e.*, the ratio of the number of in-cache embeddings to the total number of embeddings, ranges from 4% to 10%. Fig. 8 shows that ESD preserves the performance superiority over LAIA and the speedup for the same α does not vary a lot across different sizes of embedding cache. This experiment verifies the consistent effectiveness of ESD under different cache ratios.

Embedding Size. Embedding size *i.e.*, the dimension of the embedding vector, is an important factor affecting the performance of DLRM model. As shown in Fig. 9, we test the speedup and cost reduction variations of ESD($\alpha = 1$), ESD($\alpha = 0.5$), and ESD($\alpha = 0$) for embedding sizes of 128, 256, 512, and 1024. When the embedding size increases, as shown in Fig. 9a, the speedup of all three mechanisms compared to LAIA increases, reaching up to $1.59\times$. The reason is that as the embedding size increases, the data size of each embedding pull and push increases, *i.e.*, D_{tran} becomes larger,

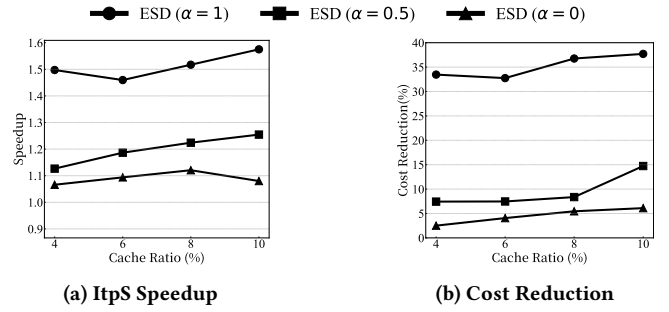


Figure 8: Impact of cache ratio.

thereby increasing the embedding transmission cost. When the transmission cost of each embedding increases, the effectiveness of ESD becomes more pronounced. For cost reduction, changes in embedding size only affect D_{tran} and do not impact the cost reduction of ESD($\alpha = 1$), ESD($\alpha = 0.5$), and ESD($\alpha = 0$) relative to LAIA. For instance, when the embedding size increases from 256 to 512, D_{tran} doubles, causing the embedding transmission cost for both LAIA and ESD to double as well. However, the relative cost reduction of LAIA remains unchanged.

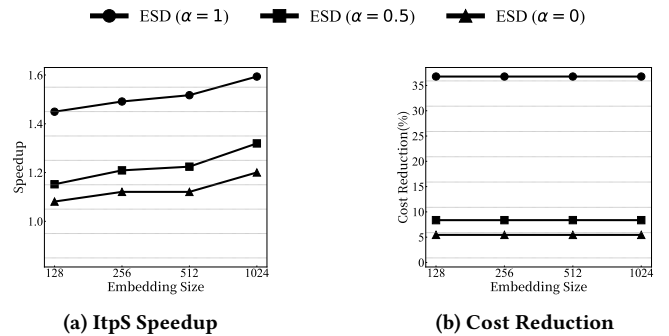


Figure 9: Impact of embedding size.

Worker Number and Network Bandwidths.

Previous experiments were conducted with 8 edge workers where the network bandwidth between workers and the PS is heterogeneous. To verify the effectiveness of ESD with different numbers of workers and with homogeneous network bandwidth between workers and the PS, we tested the performance of ESD($\alpha = 1$), ESD($\alpha = 0.5$), and ESD($\alpha = 0$) under the following settings: 1) Using four edge workers, with two 5 Gbps workers and two 0.5 Gbps workers. 2) Using four 5 Gbps workers. The experimental results are shown in Fig. 10. Under two settings, for the three mechanisms and three workloads, the speedup ranges from $1.07\times$ to $1.31\times$ and $1.03\times$ to $1.23\times$, respectively. For cost reduction, when using two 5 Gbps workers and two 0.5 Gbps workers, the cost reduction ranges from 6.06% to 42.15%. In contrast, when using four 5 Gbps workers, the cost reduction ranges from 0.33% to 29.11%. The experiments show that ESD is effective with four workers in homogeneous networks and performs better in heterogeneous networks, aligning with our motivation.

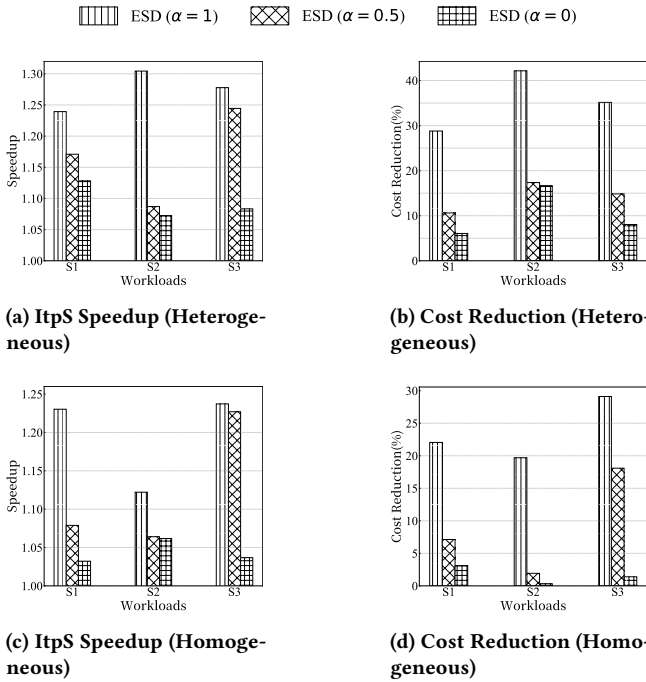


Figure 10: Experiment results when using four workers.

7 Related Works

7.1 Recommender Systems for Mobile and Ubiquitous Computing

The recommender systems designed for mobile and ubiquitous computing typically focus on privacy protection and efficiency. These systems are increasingly deployed in environments where user data is distributed across devices, such as mobile phones and edge devices, requiring approaches that reduce communication costs and respect data privacy.

HeteFedRec [77] is a federated recommendation framework that allows personalized model sizing for participants, leveraging dual-task learning for additive aggregation, dimensional decorrelation regularization to prevent collapse, and relation-based knowledge distillation to enhance knowledge sharing. Yuan *et al.* [78] propose a novel parameter transmission-free federated recommendation framework, PTF-FedRec, which facilitates collaborative learning via transmitting predictions between clients and the central server, while ensuring privacy through a sampling and swapping mechanism for local model predictions. RelayRec [15] is a privacy-preserving cloud-device relay on-device learning framework for CTR prediction, combining clustered meta-learning to train preference-specific models, an automated model selector for personalized initialization, and collaborative learning to enhance local prediction performance using decentralized private data. HFSA [35] is a semi-asynchronous hierarchical federated recommendation system that reduces communication overhead through edge aggregation, improves performance with a semi-synchronous mechanism, and ensures global model convergence by allowing slow clients to asynchronously contribute their parameters, making it suitable for dynamic mobile and edge environments. DualRec [82] is a novel collaborative training framework that combines federated learning

with efficient model aggregation and denoising mechanisms, allowing devices to train lightweight models with local data while a larger model is trained on the cloud, enhancing recommendation system performance by generating pseudo user interactions and distilling knowledge between the device and cloud models. PREFER [25] is an edge-accelerated federated learning framework for Point-of-Interest recommendation, where user-independent parameters are shared among users and aggregated on edge servers. PEPPER [7] is a decentralized recommender system based on gossip learning principles, enabling users to train personalized models asynchronously. This paper focuses on providing recommendation services for mobile and ubiquitous applications, emphasizing the improvement of training efficiency for deep learning recommendation models with huge embedding tables in edge environments. It accelerates model training by reducing embedding transmission costs through embedding samples dispatching, making it suitable for resource-limited devices in mobile and ubiquitous computing scenarios.

7.2 Accelerate Deep Learning Recommendation Models Training

Part of prior works focuses on minimizing the number of necessary transmissions [4, 37, 45]. FAE [4] decreases embedding transfers from CPUs to GPUs by storing popular embeddings on GPUs. Persia [37] advocates mixing the synchronous and asynchronous mechanisms to update MLP and embedding tables, respectively. HET [45] develops a caching consistency model that allows staleness in cache read and write operations to minimize transmission overhead, while LAIA [79] schedules embeddings to reduce transmission cost without sacrificing accuracy. Other efforts focus on reducing per-transmission latency. Ugache [58] introduces a decomposition extraction mechanism to prevent bandwidth congestion and utilizes NVLink and NVSwitch to accelerate remote GPU memory access. AdaEmbed [32] and CAFE [81] aim to reduce the transmission cost of embeddings by compressing and pruning embeddings. ScaleFreeCTR [23] employs a mixcache mechanism to eliminate transmission cost between hosts and GPUs, and leverages virtual sparse ID to reduce transmission volume. In this paper, we focus on training DLRM in edge environments. We propose ESD to address the unique challenges of edge environments, such as limited resources and heterogeneous networks, to minimize the total embedding transmission cost and thus accelerate DLRM training.

8 Discussion

8.1 Cache Replacement Policy

During the training of DLRM, when the embedding cache reaches capacity, one or more cached embeddings must be evicted to accommodate new ones. Under on-demand synchronization, if the gradients of the evicted embeddings have not yet been synchronized with the PS, an evict push operation is triggered. In this work, we design Emark, a marking-based policy to manage cached embeddings in each worker to reduce the number of evict push operations, considering recency, frequency, and the version of embedding. When embedding id x_i is dispatched to w_i , Emark assigns a mark (target) to $Emb(x_i)$, target is a positive integer starting at 1. When the cache is full, and all embeddings' marks are target,

`target` + = 1. For cache replacement, when the cache is full, `Emark` first evicts outdated embeddings, then compares marks in ascending order, and finally compares access frequency. In our implementation, we overload the `<` operator in C++ to achieve this, with the latest version marked as 1 and the outdated version as 0. Additionally, by adjusting the increment method for `target` and the comparison order in the overloaded `<` operator, `Emark` can easily adapt to different priority settings among frequency, recency, and version. Since Fig. 5b shows that evict push contributes less than 10% of transmission operation, we discuss the cache replacement policy here rather than in Sec. 4. Additionally, incorporating the embedding eviction and replacement policy into calculating the expected transmission cost is an effective way to reduce evict push operations, and we leave it for future work.

8.2 Non-uniform Embedding Size

In this paper, we propose ESD to dispatch input embedding samples to workers based on calculating the expected transmission cost under the assumption of uniform embedding vector dimensions (*i.e.*, embedding size). However, recent trends indicate the use of non-uniform embedding sizes to reduce the memory footprint, training time, and inference time of DLRM [32, 42, 86]. When embedding sizes are non-uniform, ESD can effectively handle this through the following adjustments. First, for calculating the expected transmission cost, different data sizes (D_{tran}) can be used to account for varying embedding dimensions. Secondly, regarding the cache replacement policy, non-uniform embedding sizes result in differing memory footprints within the embedding cache. This can be managed using a priority metric. The priority for each embedding in the cache is calculated by the frequency, recency, and version (latest or outdated) as the numerator, while the memory footprint of each embedding serves as the denominator. When the cache reaches capacity, embeddings with the lowest priorities are evicted first. A future direction is to explore embedding size configurations for training and deploying DLRM in edge environments.

9 Conclusion

Training and deploying DLRM on edge workers is an effective way to deliver recommendation services for modern mobile and ubiquitous applications while ensuring privacy protection and low latency. This paper focuses on dispatching input embedding samples based on expected embedding transmission costs to minimize the total embedding transmission cost. We highlight the challenges of designing a dispatch mechanism in edge environments, including cost composition, heterogeneous networks, and limited resources. To address these challenges, we propose a dispatch mechanism called ESD, incorporating a hybrid decision-making method `HybridDis` as a key component. We implement ESD using C++ (including CUDA) and Python and conduct experiments on edge workers with typical workloads to validate the improvement over the state-of-the-art mechanism. Building an efficient system for modern mobile and ubiquitous applications requires optimization in data collection, processing, model training, deploying, and more. We hope this work contributes a step towards building an efficient recommender system for mobile and ubiquitous computing. This work does not raise any ethical issues.

References

[1] Click-through rate prediction, 2024. <https://www.kaggle.com/c/avazu-ctr-prediction>.

[2] Display advertising challenge, 2024. <https://www.kaggle.com/c/criteo-display-ad-challenge>.

[3] Bilge Acun, Matthew Murphy, Xiaodong Wang, Jade Nie, Carole-Jean Wu, and Kim Hazelwood. Understanding training efficiency of deep learning recommendation models at scale. In *IEEE HPCA*, pages 802–814, 2021.

[4] Muhammad Adnan, Yassaman Ebrahizadeh Maboud, Divya Mahajan, and Prashant J Nair. Accelerating recommendation system training by leveraging popular choices. *Proceedings of the VLDB Endowment*, 15(1):127–140, 2021.

[5] Muhammad Adnan, Yassaman Ebrahizadeh Maboud, Divya Mahajan, and Prashant J Nair. Heterogeneous acceleration pipeline for recommendation system training. In *ACM/IEEE ISCA*, pages 1063–1079, 2024.

[6] Saurabh Agarwal, Chengpo Yan, Ziyi Zhang, and Shivaram Venkataraman. Bag-pipe: Accelerating deep recommendation model training. In *ACM SOSP*, pages 348–363, 2023.

[7] Yacine Belal, Aurélien Bellet, Sonia Ben Mokhtar, and Vlad Nitu. Pepper: Empowering user-centric recommender systems over gossip learning. *Proceedings of the ACM on Interactive, Mobile, Wearable and Ubiquitous Technologies*, 6(3):1–27, 2022.

[8] Maximilian Boeker and Aleksandra Urman. An empirical investigation of personalization factors on tiktok. In *ACM WWW*, pages 2298–2309, 2022.

[9] Qiqi Cai, Jian Cao, Guandong Xu, and Nengjun Zhu. Distributed recommendation systems: Survey and research directions. *ACM Transactions on Information Systems*, 43(1):1–38, 2024.

[10] Cheng Chen, Yilin Wang, Jun Yang, Yiming Liu, Mian Lu, Zhao Zheng, Bing-sheng He, Weng-Fai Wong, Liang You, Penghao Sun, et al. Openembedding: A distributed parameter server for deep learning recommendation models using persistent memory. In *IEEE ICDE*, pages 2976–2987, 2023.

[11] Wenqiang Chen, Lizhang Zhan, Yuanlong Ci, Minghua Yang, Chen Lin, and Dugang Liu. Flen: leveraging field for scalable ctr prediction. *arXiv preprint arXiv:1911.04690*, 2019.

[12] Heng-Tze Cheng, Levent Koc, Jeremiah Harmsen, Tal Shaked, Tushar Chandra, Hrishi Aradhye, Glen Anderson, Greg Corrado, Wei Chai, Mustafa Ispir, et al. Wide & deep learning for recommender systems. In *Proceedings of the 1st workshop on deep learning for recommender systems*, pages 7–10, 2016.

[13] Paul Covington, Jay Adams, and Emre Sargin. Deep neural networks for youtube recommendations. In *ACM RecSys*, pages 191–198, 2016.

[14] Paul Delestrac, Debjyoti Battacharjee, Simei Yang, Diksha Moolchandani, Francky Catthoor, Lionel Torres, and David Novo. Multi-level analysis of gpu utilization in ml training workloads. In *2024 Design, Automation & Test in Europe Conference & Exhibition (DATE)*, pages 1–6. IEEE, 2024.

[15] Yongheng Deng, Guanbo Wang, Sheng Yue, Wei Rao, Qin Zu, Wenjie Wang, Shuai Chen, Ju Ren, and Yaoxue Zhang. Relayrec: Empowering privacy-preserving ctr prediction via cloud-device relay learning. In *ACM/IEEE IPSN*, pages 188–199. IEEE, 2024.

[16] Yuchen Ding, Siqing Zhang, Boyu Fan, Wei Sun, Yong Liao, and Peng Yuan Zhou. Fedloca: Low-rank coordinated adaptation with knowledge decoupling for federated recommendations. In *ACM RecSys*, pages 690–700, 2024.

[17] Ye Gao, Meiyi Ma, Kristina Gordon, Karen Rose, Hongning Wang, and John Stankovic. A monitoring, modeling, and interactive recommendation system for in-home caregivers: Demo abstract. In *ACM SenSys*, pages 587–588, 2020.

[18] Saeed Ghadimi, Guanghui Lan, and Hongchao Zhang. Mini-batch stochastic approximation methods for nonconvex stochastic composite optimization. *Mathematical Programming*, 155(1):267–305, 2016.

[19] Carlos A Gomez-Uribe and Neil Hunt. The netflix recommender system: Algorithms, business value, and innovation. *ACM Transactions on Management Information System*, 6(4):1–19, 2015.

[20] Yu Gong, Ziwen Jiang, Yufei Feng, Binbin Hu, Kaiqi Zhao, Qingwen Liu, and Wenwu Ou. Edgerec: recommender system on edge in mobile taobao. In *ACM CIKM*, pages 2477–2484, 2020.

[21] Priya Goyal, Piotr Dollar, Ross Girshick, Pieter Noordhuis, Lukasz Wesolowski, Aapo Kyrola, Andrew Tulloch, Yangqing Jia, and Kaiming He. Accurate, large minibatch sgd: Training imagenet in 1 hour. *arXiv preprint arXiv:1706.02677*, 2017.

[22] Yulong Gu, Wentian Bao, Dan Ou, Xiang Li, Baoliang Cui, Biyu Ma, Haikuan Huang, Qingwen Liu, and Xiaoyi Zeng. Self-supervised learning on users' spontaneous behaviors for multi-scenario ranking in e-commerce. In *ACM CIKM*, pages 3828–3837, 2021.

[23] Hui Feng Guo, Wei Guo, Yong Gao, Ruiming Tang, Xiuqiang He, and Wenzhi Liu. Scalefreetr: Mixcache-based distributed training system for ctr models with huge embedding table. In *ACM SIGIR*, pages 1269–1278, 2021.

[24] Hui Feng Guo, Ruiming Tang, Yuning Ye, Zhenguo Li, and Xiuqiang He. Deepfm: a factorization-machine based neural network for ctr prediction. *arXiv preprint arXiv:1703.04247*, 2017.

[25] Yeting Guo, Fang Liu, Zhiping Cai, Hui Zeng, Li Chen, Tongqing Zhou, and Nong Xiao. Prefer: Point-of-interest recommendation with efficiency and privacy-preservation via federated edge learning. *Proceedings of the ACM on Interactive, Mobile, Wearable and Ubiquitous Technologies*, 5(1):1–25, 2021.

[26] Yassine Himeur, Abdullah Alsalem, Ayman Al-Kababji, Faycal Bensaali, Abbes Amira, Christos Sardianos, George Dimitrakopoulos, and Iraklis Varlamis. A survey of recommender systems for energy efficiency in buildings: Principles, challenges and prospects. *Information Fusion*, 72:1–21, 2021.

[27] Yassine Himeur, Shahab Saquib Sohail, Faycal Bensaali, Abbes Amira, and Mamoun Alazab. Latest trends of security and privacy in recommender systems: a comprehensive review and future perspectives. *Computers & Security*, 118:102746, 2022.

[28] Jiazhai Jiang, Rui Tian, Jiangsu Du, Dan Huang, and Yutong Lu. Mixrec: Orchestrating concurrent recommendation model training on cpu-gpu platform. In *IEEE ICCD*, pages 366–374, 2023.

[29] Z Jonny Kong, Qiang Xu, Jiayi Meng, and Y Charlie Hu. Accumo: Accuracy-centric multitask offloading in edge-assisted mobile augmented reality. In *ACM MobiCom*, pages 1–16, 2023.

[30] Harold W Kuhn. The hungarian method for the assignment problem. *Naval research logistics quarterly*, 2(1-2):83–97, 1955.

[31] Youngeun Kwon and Minsoo Rhu. Training personalized recommendation systems from gpu scratch: Look forward not backwards. In *ACM/IEEE ISCA*, pages 860–873, 2022.

[32] Fan Lai, Wei Zhang, Rui Liu, William Tsai, Xiaohan Wei, Yuxi Hu, Sabin Devkota, Jianyu Huang, Jongsoo Park, Xing Liu, et al. Adaembed: Adaptive embedding for large-scale recommendation models. In *USENIX OSDI*, pages 817–831, 2023.

[33] Eugene L Lawler. *Combinatorial optimization: networks and matroids*. Courier Corporation, 1976.

[34] Jiayu Li, Zhiyu He, Yumeng Cui, Chenyang Wang, Chong Chen, Chun Yu, Min Zhang, Yiqun Liu, and Shaoping Ma. Towards ubiquitous personalized music recommendation with smart bracelets. *Proceedings of the ACM on Interactive, Mobile, Wearable and Ubiquitous Technologies*, 6(3):1–34, 2022.

[35] Youhuizi Li, Haitao Yu, Yan Zeng, and Qianqian Pan. Hfsa: A semi-asynchronous hierarchical federated recommendation system in smart city. *IEEE Internet of Things Journal*, 10(21):18808–18820, 2023.

[36] Yun Li, Hui Ma, Lei Wang, Shiven Mao, and Guoyin Wang. Optimized content caching and user association for edge computing in densely deployed heterogeneous networks. *IEEE Transactions on Mobile Computing*, 21(6):2130–2142, 2020.

[37] Xiangru Lian, Binhang Yuan, Xuefeng Zhu, Yulong Wang, Yongjun He, Honghuan Wu, Lei Sun, Haodong Lyu, Chengjun Liu, Xing Dong, et al. Persia: An open, hybrid system scaling deep learning-based recommenders up to 100 trillion parameters. In *ACM SIGKDD*, pages 3288–3298, 2022.

[38] Neiwen Ling, Kai Wang, Yuze He, Guoliang Xing, and Daqi Xie. Rt-mdl: Supporting real-time mixed deep learning tasks on edge platforms. In *ACM SenSys*, pages 1–14, 2021.

[39] Jing Long, Tong Chen, Quoc Viet Hung Nguyen, and Hongzhi Yin. Decentralized collaborative learning framework for next poi recommendation. *ACM Transactions on Information Systems*, 41(3):1–25, 2023.

[40] Jing Long, Guanhua Ye, Tong Chen, Yang Wang, Meng Wang, and Hongzhi Yin. Diffusion-based cloud-edge-device collaborative learning for next poi recommendations. In *ACM SIGKDD*, pages 2026–2036, 2024.

[41] Paulo AC Lopes, Satyendra Singh Yadav, Aleksandar Ilic, and Sarat Kumar Patra. Fast block distributed cuda implementation of the hungarian algorithm. *Journal of Parallel and Distributed Computing*, 130:50–62, 2019.

[42] Qinyi Luo, Penghan Wang, Wei Zhang, Fan Lai, Jiachen Mao, Xiaohan Wei, Jun Song, Wei-Yu Tsai, Shuai Yang, Yuxi Hu, et al. Fine-grained embedding dimension optimization during training for recommender systems. *arXiv preprint arXiv:2401.04408*, 2024.

[43] Kaihao Ma, Xiao Yan, Zhenkun Cai, Yuzhen Huang, Yidi Wu, and James Cheng. Fec: Efficient deep recommendation model training with flexible embedding communication. *Proceedings of the ACM on Management of Data*, 1(2):1–21, 2023.

[44] Kiran Kumar Matam, Hani Ramezani, Fan Wang, Zeliang Chen, Yue Dong, Maomao Ding, Zhiwei Zhao, Zhengyu Zhang, Ellie Wen, and Assaf Eiseman. Quickupdate: a real-time personalization system for large-scale recommendation models. In *USENIX NSDI*, pages 731–744, 2024.

[45] Xupeng Miao, Hailin Zhang, Yining Shi, Xiaonan Nie, Zhi Yang, Yangyu Tao, and Bin Cui. Het: scaling out huge embedding model training via cache-enabled distributed framework. *Proceedings of the VLDB Endowment*, 15(2):312–320, 2021.

[46] Khalil Muhammad, Qinjin Wang, Diarmuid O'Reilly-Morgan, Elias Tragos, Barry Smyth, Neil Hurley, James Geraci, and Aonghus Lawlor. Fedfast: Going beyond average for faster training of federated recommender systems. In *ACM SIGKDD*, pages 1234–1242, 2020.

[47] James Munkres. Algorithms for the assignment and transportation problems. *Journal of the society for industrial and applied mathematics*, 5(1):32–38, 1957.

[48] Chanwon Park and Jemin Lee. Mobile edge computing-enabled heterogeneous networks. *IEEE Transactions on Wireless Communications*, 20(2):1038–1051, 2020.

[49] Adam Paszke, Sam Gross, Francisco Massa, Adam Lerer, James Bradbury, Gregory Chanan, Trevor Killeen, Zeming Lin, Natalia Gimelshein, Luca Antiga, et al. Pytorch: An imperative style, high-performance deep learning library. In *NeurIPS*, 2019.

[50] Farhad Pourpanah and Ali Etemad. Exploring the landscape of ubiquitous in-home health monitoring: a comprehensive survey. *ACM Transactions on Computing for Healthcare*, 5(4):1–43, 2024.

[51] Haidong Rong, Yangzihao Wang, Feihu Zhou, Junjie Zhai, Haiyang Wu, Rui Lan, Fan Li, Han Zhang, Yuekui Yang, Zhenyu Guo, et al. Distributed equivalent substitution training for large-scale recommender systems. In *ACM SIGIR*, pages 911–920, 2020.

[52] Aya Sayed, Yassine Himeur, Abdullah Alsailemi, Faycal Bensaali, and Abbes Amira. Intelligent edge-based recommender system for internet of energy applications. *IEEE Systems Journal*, 16(3):5001–5010, 2021.

[53] Markus Schedl, Peter Knees, and Fabien Gouyon. New paths in music recommender systems research. In *ACM RecSys*, pages 392–393, 2017.

[54] Aneesh Sharma, Jerry Jiang, Praveen Bommannavar, Brian Larson, and Jimmy Lin. Graphjet: Real-time content recommendations at twitter. *Proceedings of the VLDB Endowment*, 9(13):1281–1292, 2016.

[55] Sudipta Saha Shubha, Haiying Shen, and Anand Iyer. Usher: Holistic interference avoidance for resource optimized ml inference. In *USENIX OSDI*, pages 947–964, 2024.

[56] Chijun Sima, Yao Fu, Man-Kit Sit, Liyi Guo, Xuri Gong, Feng Lin, Junyu Wu, Yongsheng Li, Haidong Rong, Pierre-Louis Aublin, et al. Ekko: A large-scale deep learning recommender system with low-latency model update. In *USENIX OSDI*, pages 821–839, 2022.

[57] Brent Smith and Greg Linden. Two decades of recommender systems at amazon.com. *IEEE Internet Computing*, 21(3):12–18, 2017.

[58] Xiaoniu Song, Yiwen Zhang, Rong Chen, and Haibo Chen. Ugache: A unified gpu cache for embedding-based deep learning. In *ACM SOSP*, pages 627–641, 2023.

[59] Xin Su, Giancarlo Sperli, Vincenzo Moscato, Antonio Picariello, Christian Esposito, and Chang Choi. An edge intelligence empowered recommender system enabling cultural heritage applications. *IEEE Transactions on Industrial Informatics*, 15(7):4266–4275, 2019.

[60] Zehua Sun, Yonghui Xu, Yong Liu, Wei He, Lanju Kong, Fangzhao Wu, Yali Jiang, and Lizhen Cui. A survey on federated recommendation systems. *IEEE Transactions on Neural Networks and Learning Systems*, 2024.

[61] Marcelo Tallis and Pranjal Yadav. Reacting to variations in product demand: An application for conversion rate (cr) prediction in sponsored search. In *IEEE Big Data*, pages 1856–1864, 2018.

[62] Taegeon Um, Byungssoo Oh, Minyoung Kang, Woo-Yeon Lee, Goeun Kim, Dongseob Kim, Youngtaek Kim, Mohd Muzzammil, and Myeongjae Jeon. Metis: Fast automatic distributed training on heterogeneous gpus. In *USENIX ATC*, pages 563–578, 2024.

[63] Chunnan Wang, Hongzhi Wang, Junzhe Wang, and Guosheng Feng. Autosr: Automatic sequential recommendation system design. *IEEE Transactions on Knowledge and Data Engineering*, 2024.

[64] Jizhe Wang, Pipei Huang, Huan Zhao, Zhibo Zhang, Binqiang Zhao, and Dik Lun Lee. Billion-scale commodity embedding for e-commerce recommendation in alibaba. In *ACM SIGKDD 2018*, pages 839–848, 2018.

[65] Qinyong Wang, Hongzhi Yin, Tong Chen, Zi Huang, Hao Wang, Yanchang Zhao, and Nguyen Quoc Viet Hung. Next point-of-interest recommendation on resource-constrained mobile devices. In *ACM WWW*, pages 906–916, 2020.

[66] Ruoxi Wang, Bin Fu, Gang Fu, and Mingliang Wang. Deep & cross network for ad click predictions. In *ADKDD*, pages 1–7, 2017.

[67] Siqi Wang, Tianyu Feng, Hailong Yang, Xin You, Bangduo Chen, Tongxuan Liu, Zhongzhi Luan, and Depei Qian. Atrec: Accelerating recommendation model training on cpus. *IEEE Transactions on Parallel and Distributed Systems*, 2024.

[68] Zheng Wang, Yuke Wang, Jiaqi Deng, Di Zheng, Ang Li, and Yufei Ding. Rap: Resource-aware automated gpu sharing for multi-gpu recommendation model training and input preprocessing. In *ACM ASPLOS*, pages 964–979, 2024.

[69] Yingcan Wei, Matthias Langer, Fan Yu, Minseok Lee, Jie Liu, Ji Shi, and Zehuan Wang. A gpu-specialized inference parameter server for large-scale deep recommendation models. In *ACM RecSys*, 2022.

[70] Stephen Xia, Peter Wei, Yanchen Liu, Andrew Sonta, and Xiaofan Jiang. Reca: A multi-task deep reinforcement learning-based recommender system for co-optimizing energy, comfort and air quality in commercial buildings. In *Proceedings of the 10th ACM International Conference on Systems for Energy-Efficient Buildings, Cities, and Transportation*, pages 99–109, 2023.

[71] Minhui Xie, Youyou Lu, Qing Wang, Yangyang Feng, Jiaqiang Liu, Kai Ren, and Jiwu Shu. Petps: Supporting huge embedding models with persistent memory. *Proceedings of the VLDB Endowment*, 16(5):1013–1022, 2023.

[72] Chen Yang, Jin Chen, Qian Yu, Xiangdong Wu, Kui Ma, Zihao Zhao, Zhiwei Fang, Wenlong Chen, Chaosheng Fan, Jie He, et al. An incremental update framework for online recommenders with data-driven prior. In *ACM CIKM*, pages 4894–4900, 2023.

[73] Hongzhi Yin, Tong Chen, Liang Qu, and Bin Cui. On-device recommender systems: A tutorial on the new-generation recommendation paradigm. In *ACM WWW*, pages 1280–1283, 2024.

[74] Rex Ying, Ruining He, Kaifeng Chen, Pong Eksombatchai, William L Hamilton, and Jure Leskovec. Graph convolutional neural networks for web-scale recommender systems. In *ACM SIGKDD*, pages 974–983, 2018.

[75] Keping Yu, Zhiwei Guo, Yu Shen, Wei Wang, Jerry Chun-Wei Lin, and Takuro Sato. Secure artificial intelligence of things for implicit group recommendations. *IEEE Internet of Things Journal*, 9(4):2698–2707, 2021.

[76] Yongbo Yu, Fuxun Yu, Xiang Sheng, Chenchen Liu, and Xiang Chen. Eaglerec: Edge-scale recommendation system acceleration with inter-stage parallelism optimization on gpus. In *ACM/IEEE DAC*, pages 1–6, 2023.

[77] Wei Yuan, Liang Qu, Lizhen Cui, Yongxin Tong, Xiaofang Zhou, and Hongzhi Yin. Hetefedrec: Federated recommender systems with model heterogeneity. In *IEEE ICDE*, pages 1324–1337, 2024.

[78] Wei Yuan, Chaoqun Yang, Liang Qu, Quoc Viet Hung Nguyen, Jianxin Li, and Hongzhi Yin. Hide your model: A parameter transmission-free federated recommender system. In *2024 IEEE ICDE*, pages 611–624. IEEE, 2024.

[79] Chaoliang Zeng, Xudong Liao, Xiaodian Cheng, Han Tian, Xincheng Wan, Hao Wang, and Kai Chen. Accelerating neural recommendation training with embedding scheduling. In *USENIX NSDI*, pages 1141–1156, 2024.

[80] Chunxu Zhang, Guodong Long, Tianyi Zhou, Zijian Zhang, Peng Yan, and Bo Yang. Gpfedrec: Graph-guided personalization for federated recommendation. In *ACM SIGKDD*, pages 4131–4142, 2024.

[81] Hailin Zhang, Zirui Liu, Boxuan Chen, Yikai Zhao, Tong Zhao, Tong Yang, and Bin Cui. Cafe: Towards compact, adaptive, and fast embedding for large-scale recommendation models. *Proceedings of the ACM on Management of Data*, 2(1):1–28, 2024.

[82] Ye Zhang, Yongheng Deng, Sheng Yue, Qiushi Li, and Ju Ren. Dualrec: A collaborative training framework for device and cloud recommendation models. *IEEE Transactions on Mobile Computing*, 2025.

[83] Yuanxing Zhang, Langshi Chen, Siran Yang, Man Yuan, Huimin Yi, Jie Zhang, Jiamang Wang, Jianbo Dong, Yunlong Xu, Yue Song, et al. Picasso: Unleashing the potential of gpu-centric training for wide-and-deep recommender systems. In *IEEE ICDE 2022*, pages 3453–3466, 2022.

[84] Mark Zhao, Dhruv Choudhary, Devasish Tyagi, Ajay Soman, Max Kaplan, Sung-Han Lin, Sarunya Pumma, Jongsoo Park, Aarti Basant, Niket Agarwal, et al. Recd: Deduplication for end-to-end deep learning recommendation model training infrastructure. In *MLSys 2023*, pages 754–767, 2023.

[85] Xiangyu Zhao, Maolin Wang, Xinjian Zhao, Jiansheng Li, Shucheng Zhou, Dawei Yin, Qing Li, Jiliang Tang, and Ruocheng Guo. Embedding in recommender systems: A survey. *arXiv preprint arXiv:2310.18608*, 2023.

[86] Xiangyu Zhao, Haochen Liu, Wenqi Fan, Hui Liu, Jiliang Tang, Chong Wang, Ming Chen, Xudong Zheng, Xiaobing Liu, and Xiwang Yang. Autoemb: Automated embedding dimensionality search in streaming recommendations. In *IEEE ICDM*, pages 896–905, 2021.

[87] Guorui Zhou, Xiaoqiang Zhu, Chenru Song, Ying Fan, Han Zhu, Xiao Ma, Yanghui Yan, Junqi Jin, Han Li, and Kun Gai. Deep interest network for click-through rate prediction. In *ACM SIGKDD 2018*, pages 1059–1068, 2018.